Supplementary material

Protective recommendations for non-invasive ventilation during COVID-19 pandemic: a bench evaluation of the effects of instrumental dead space on alveolar ventilation.

Mathieu DELORME, PT, MSc; Karl LEROUX; Ghilas BOUSSAID, PT, PhD; Marius LEBRET, PT, PhD; Helene PRIGENT, MD, PhD; Antoine LEOTARD, MD; Bruno LOUIS, PhD; Frédéric LOFASO, MD, PhD.

SUPPLEMENTARY METHODS

Respiratory system model

The test lung used was a dual-chamber Michigan test lung (MII Vent Aid TTL; Michigan Instrument, Grand Rapids, MI, USA). The two chambers of the test-lung were connected with each other by a fixed metal component and connected to the rest of the set up through a Y-piece so that both chambers lifted and dropped synchronously during ventilation. The compliance of each chamber was seat at 30 mL/cmH_2O. The two chambers were joined on the same limb connected successively to a linear resistor (5 cmH_2O/L/sec) (Pneuflo® Airway resistor Rp5; Michigan Instrument, Grand Rapids, MI, USA), a flow sensor, a pressure sensor, a capnometer, and an adult-sized mannequin head (Supplementary Figure 1).

Data acquisition

Respiratory flow (V'_{aw}) was measured between the mannequin head and the test lung using a pneumotachograph (Fleish #2; Lausanne, Switzerland) connected to a differential pressure transducer (Validyne DP45±2.25 cm H_2O; Northridge, CA, USA). At the same site, airway pressure (P_{aw}) was measured with another differential pressure transducer (Validyne DP45±56 cm H_2O). CO_2 flow was measured using a pneumotachograph (Fleish #0000; Lausanne, Switzerland) associated with a differential pressure transducer (Validyne DP45 ±2.25 cm H_2O; Northridge, CA, USA). Partial pressure of CO_2 (PCO_2) was continuously monitored with a mainstream CO_2 analyzer (Capnogard 1265; Novametrix, USA) (Supplementary Figure 1). Sensors were calibrated according to manufacturers' recommendations before

experimentation. Signals were digitized at 200 Hz by an analogical/digital system (MP100, Biopac Systems, Goleta, CA, USA) and recorded on a microcomputer for further analysis.

The additional VD with the different configurations evaluated was calculated according to Bohr's equation ($P_{ET}CO_2 = V'CO_2 \times 0.863 / V'A$), where $V'CO_2$ is the measured CO_2 inflow into the test lung (in mL/min) and V'A represents alveolar ventilation. V'A corresponds to RR x (VT_E–VD) where RR represents respiratory rate, VT_E is the calculated expired tidal volume (mL) and VD represents the total dead space (mL), including both anatomical and instrumental dead spaces. Accordingly, by adjusting VT_E to obtain a constant $P_{ET}CO_2$ in the different circuit conditions, while $V'CO_2$ and RR remained constant, we obviously maintained the same (VT_E–VD). From these equations, we were able to determine the additional dead spaces with the different configurations evaluated, which are reported in the results section of the manuscript and are consistent with VT_E variations at iso-$P_{ET}CO_2$.

Additional measurements were performed to determine circuit compliance and resistances according to the different configurations evaluated.

Compliance was determined for all configurations by increasing the volume of the circuit closed with a cap by 5, 10, 15 and 20 mL (ΔV) with the help of a calibrated syringe. Simultaneous recording of pressure variations (ΔP) inside the circuit allowed to calculate $\Delta V/\Delta P$ ratio at each point of measurement. Relationship between volume and pressure variations for this range of measurements was linear for all circuits, and we therefore calculated mean compliance of the circuits (in mL/cmH_2O) for each configuration.

Resistances were calculated both during inspiration and expiration. Inspiratory resistance was determined with the distal part of the circuit opened to the atmosphere. For configurations E and F, expiratory limb of the circuit was occluded during the procedure. A calibrated flow generator was used to increase inspiratory flow inside the circuit. Pressure and flow variations were monitored at the proximal part of the circuit (ventilator side) to determine inspiratory resistance (in cmH_2O/L/sec). Conversely, expiratory resistance was determined by generating a calibrated expiratory flow from the test lung to the interface, with pressure and flow variations monitored inside the mask. For each configuration, the inspiratory limb of

the circuit and the anti-asphyxia system of the leak were closed so that exhalation could only occur through the calibrated intentional leak (for configurations A to D) or through the expiratory limb of the circuit (for configuration E and F).

Particular attention was paid to ensure no extra-leak occurred between the mask and the mannequin head during these measurements. Pressure – flow diagrams were recorded for each procedure. Mean pressure drop at 0.5 L/sec was calculated and both inspiratory and expiratory resistances are presented in $cmH_2O/L/sec$.

SUPPLEMENTARY RESULTS

Supplementary Table 1. Circuit compliance, inspiratory and expiratory resistances according to the different configurations evaluated.

Variables	Config. A	Config. B	Config. C	Config. D	Config. E	Config. F
Compliance (mL/cmH_2O)	0.4	0.6	0.6	0.7	1.5	2.2
Inspiratory resistance* (cmH_2O/L/sec)	2.0	2.1	1.4	2.0	2.2	3.3
Expiratory resistance* (cmH_2O/L/sec)	3.3	18.5	19.1	20.0	2.2	4.0

* Inspiratory and expiratory resistances were calculated at 0.5 L/sec, and expressed in cmH_2O/L/sec.

SUPPLEMENTARY FIGURES

Supplementary Figure 1. Illustration of the experimental setup

A test lung was used to simulate patient's respiratory mechanics with compliance 60 mL/cmH_2O and resistance 5 cmH_2O/L/sec. Constant flow of 100% CO_2 (V'CO_2) was provided into the test lung (180±5 mL/min). An adult-sized mannequin head was connected to the test lung. Respiratory flow (V'aw), airway pressure (Paw) and CO_2 partial pressure (PCO_2) were continuously monitored between the mannequin head and test lung. The mannequin head was connected to the ventilator through the different configurations evaluated.

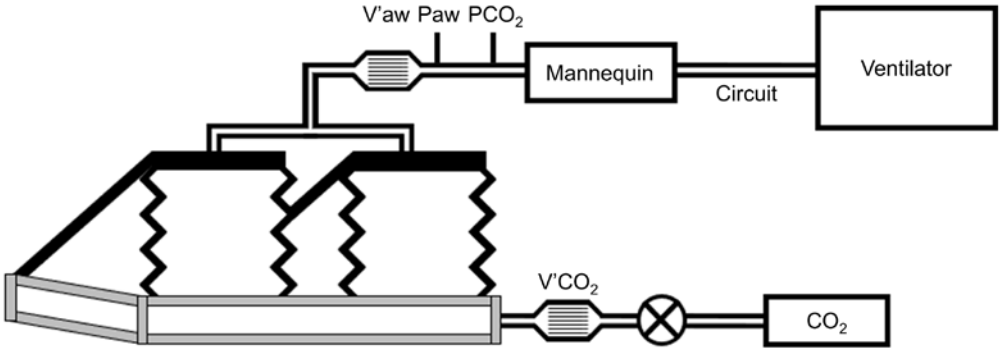

Supplementary Figure 2. Pressure – Flow relationship according to the different configurations evaluated

The diagrams represent the pressure – flow relationship for the different conditions evaluated during inspiration (panel A) and expiration (panel B). Note the modification of the scale on the Y-axis between panels A et B.